Journal of Colloid and Interface Science 369 (2012) 238–244

Contents lists available at SciVerse ScienceDirect

Journal of Colloid and Interface Science

www.elsevier.com/locate/jcis

Hydrotropic salt promotes anionic surfactant self-assembly into vesicles and ultralong fibers

Yiyang Lin [a], Yan Qiao [a], Xinhao Cheng [a], Yun Yan [a], Zhibo Li [b], Jianbin Huang [a,*]

[a] Beijing National Laboratory for Molecular Sciences (BNLMS), State Key Laboratory for Structural Chemistry of Unstable and Stable Species, College of Chemistry and Molecular Engineering, Peking University, Beijing 100871, China
[b] Beijing National Laboratory for Molecular Science (BNLMS), Institute of Chemistry, Chinese Academy of Sciences, Beijing 100190, China

ARTICLE INFO

Article history:
Received 8 August 2011
Accepted 28 November 2011
Available online 6 December 2011

Keywords:
Surfactant self-assembly
Hydrotropic salt
Fiber
Vesicle

ABSTRACT

Molecular self-assembly has become a versatile approach to create complex and functional nanoarchitectures. In this work, the self-assembly behavior of an anionic surfactant (sodium dodecylbenzene sulfonate, SDBS) and a hydrotropic salt (benzylamine hydrochloride, BzCl) in aqueous solution is investigated. Benzylamine hydrochloride is found to facilitate close packing of surfactants in the aggregates, inducing the structural transformation from SDBS micelles into unilamellar vesicles, and multilamellar vesicles. The multilamellar vesicles can transform into macroscale fibers, which are long enough to be visualized by the naked eye. Particularly, these fibers are robust enough to be conveniently separated from the surfactant solution. The combined effect of non-covalent interactions (e.g., hydrophobic effect, electrostatic attractions, and π–π interactions) is supposed to be responsible for the robustness of these self-assembled aggregates, in which π–π interactions provide the directional driving force for one-dimensional fiber formation.

1. Introduction

Surfactants are known to self-assemble into diverse nanostructures (e.g., micelles, vesicles, and lamellae) in aqueous solution when the surfactant concentration is above a critical micelle concentration (cmc) [1,2]. The introduction of additives such as inorganic salts, hydrotropic salts, organic additives, and oppositely charged surfactants are found to greatly promote surfactant self-assembly in water [3–10]. Particularly, hydrotropic salts are found to induce viscoelastic wormlike micelle formation in ionic surfactant solutions, in which surfactants interact strongly with hydrotropic salts owing to electrostatic attraction and hydrophobic effect. Hydrotropic salts are a class of amphiphilic compounds that cannot form aggregates, such as micelles, but do solubilize organic molecules in water [11–14]. The structural characteristics of hydrotropic salts are the coexistence of an aromatic group (hydrophobic) and an ionic group (hydrophilic) within one molecule. Salicylate [5,6,15–17], tosylate [18], dichlorobenzoate [19], hydroxynaphthalenecarboxylate [20], hydroxyl benzoate [21], benzoate [22,23], naphthalenesulfonate [24], and phthalic acid [25] are typical hydrotropic salts in surfactant solutions. Despite the number of studies dedicated to the study of surfactant/hydrotropic salt mixtures, most of the work is concentrated on the formation of viscoelastic wormlike micelle. Studies on higher ordered self-assemblies in surfactant/hydrotropic salt systems are less reported [26–28].

On the other hand, one-dimensional (1D) self-assembled nanostructures such as fibers [29], helices [30–32], and tubes [33] have received extensive attention over the past decade. This is because the beneficial influence of dimensionality on electronic, optical, and magnetic properties may endow peculiar properties and applications to 1D materials [34]. In addition, one-dimensional nanostructures play an important role in life science and biological phenomena including cell deformation and division, blood clotting, DNA double helix, and amyloid fibrils [35]. Therefore the rational design of 1D nanostructures has aroused much research interest from supramolecular chemistry, biological chemistry, and nanochemistry. Although much work has been published concerning self-assembled 1D nano/microstructures, these molecular self-assemblies in many cases have defined sizes and shapes within the nanometer-to-micrometer length scale. As a result, it remains a tough challenge to isolate self-assembled nanofibers, nanotubes, or nanobelts from supramolecular solution or gel networks, which will restrict further application of 1D structure in practical fields. It is therefore essentially important to prepare self-assembled 1D aggregate in macroscopic scale. However, such work is seldom reported still now. For example, Menger has obtained organic fibers with several centimeters long by non-covalent self-assembly of potassium 5-(hexadecyloxy) isophthalic solution, which are stabilized by hydrogen bonds and hydrophobic interactions [36]. Recently, Yan and coworkers have described macroscopic

* Corresponding author. Fax: +86 10 62751708.
E-mail address: JBHuang@pku.edu.cn (J. Huang).

0021-9797/$ - see front matter © 2011 Elsevier Inc. All rights reserved.
doi:10.1016/j.jcis.2011.11.067

self-assembly of an amphiphilic hyperbranched copolymer into multiwalled microtubes with millimeters in diameter and centimeters in length [37]. The formation of hydrogen bonds in both core and arm lamellae is supposed to drive the macroscale self-assembly process. It can be noted from the above studies that strong intermolecular interactions are indispensable to fabricate macroscale molecular self-assemblies and stabilize self-organized architectures. To satisfy this requirement, novel synthetic molecules or macromolecules modified with functional groups are usually needed which require complicated and time-consuming organic synthesis.

The aim of this work seeks to create high-ordered macroscale structures through surfactant/hydrotropic salt self-assembly. Sodium dodecylbenzene sulfonate (SDBS) and benzylamine hydrochloride (BzCl) are chosen. Compared with the reported surfactant/hydrotropic salt mixtures, the main characteristic of SDBS/BzCl is that both compounds possess phenyl rings, which may contribute to hydrophobic effect and π–π interactions. Multiple techniques including transmission electron microscopy (TEM), cryo-TEM, optical microscopy, confocal laser scanning microscopy (CLSM), X-ray diffraction (XRD), fluorescence probe technique, turbidity measurement, and ζ potential measurement are applied to characterize the self-assembly property of SDBS/BzCl. It is found that SDBS micelles transform into unilamellar and multilamellar vesicles with the addition of BzCl. Unexpectedly, multilamellar vesicles can further transform into ultralong fibers. The correlation between the fascinating self-assembly behavior and the molecular structure, especially the aromatic rings of surfactant and hydrotropic salt, will be discussed, which may provide instructions for fabricating well-ordered structures through surfactant/hydrotropic salt self-assembly.

2. Materials and methods

2.1. Materials

Sodium dodecylbenzene sulfonate (SDBS) was bought from Acros and used as received. Benzylamine hydrochloride (BzCl) was obtained from Beijing Chemical Reagents Co. and recrystallized three times from ethanol/ethyl ether. Distilled water was purified through Milli-Q Advantage A10 Ultrapure Water System with a minimum resistivity of 18.4 MΩ cm.

2.2. Sample preparation

The desired amount of SDBS and BzCl was added into deioned water and heated until the solid was completely soluble in water. After that, the surfactant solution was equilibrated at desired temperature before investigation.

2.3. UV–vis absorbance

The turbidity of surfactant solution was obtained from UV–vis absorbance measurements, which were carried out on the spectrophotometer (Cary 1E, Varian Australia PTY Ltd.) equipped with a thermostated cell holder. The UV–vis measurements were conducted at 25 °C.

2.4. Transmission electron microscopy (TEM)

A small drop of sample was placed on a 230 mesh copper grid, and the redundant liquid was blotted off with a piece of filter paper. The copper grid was then applied to TEM observation at the accelerated voltage of 120 kV. A JEM-100CX electron microscope was employed in the microscopic observation.

2.5. Cryo-transmission electron microscopy (cryo-TEM)

A small drop of sample was placed on a 400 mesh copper grid, and a thin film was produced by blotting off the redundant liquid with filter paper. This thin film was then quickly dipped into liquid ethane, which was cooled by liquid nitrogen. Observation of the cryo-sample was carried out at −183 °C.

2.6. Scanning electron microscopy (SEM)

The surfactant solution with ultralong fibers was dropped onto silicon plate and air-dried before applied to SEM observation (SEM, Hitachi S4800).

2.7. Optical microscopy

The surfactant sample was placed on a pre-cleaned glass surface, which was covered by microscope slide glass. Optical microscopy images were recorded on a Nikon ECLIPSE E600 microscope.

2.8. Confocal laser scanning microscopy (CLSM)

The CLSM observation of vesicular solution was carried out in the presence of hydrophobic dye of Nile Red, which was prepared through the following process: 10 μL stock solution of 2.5 mM Nile Red in ethanol was added to a test tube, followed by volatilization of the ethanol. Then, a desired amount of surfactant solution (1 mL) was added to the tube. All the samples were allowed for 24 h equilibrium before CLSM experiments. The solutions containing Nile Red were dropped onto a pre-cleaned glass surface, which was covered by microscope slide glass. The edge of the slide was sealed to avoid water evaporation. CLSM observation was conducted on a Leica Tcs-sp confocal laser scanning microscope.

2.9. X-ray diffraction (XRD)

The organic fibers were isolated from the surfactant solution by centrifuging and washed several times with cold deioned water. The solid was dried in vacuum and transferred to pre-cleaned glass slide. XRD study was carried out with a model XKS-2000 X-ray diffractometer (Scintaginc). The X-ray beam was generated with a Cu anode, and the wavelength of the KR1 beam was 1.5406 Å. The scanning was done up to the 2θ value of 30°.

2.10. Fluorescence measurement

Steady-state fluorescence spectra were obtained with an Edinburgh FLS920 fluorescence spectrophotometer. In these studies, a fixed amount (2.5 μM) of the fluorescent probe Nile Red was added into surfactant solution and stirred for 24 h to reach equilibrium. The excitation wavelength of Nile Red was 575 nm and the fluorescence emission was monitored.

2.11. ζ-Potential

The ζ potentials of surfactant solution were measured using a temperature-controlled ZetaSizer 2000 (Malvern Instruments Ltd.) ζ potential analyzer. Each sample was measured at least three times.

3. Results and discussion

3.1. Benzylamine hydrochloride-assisted surfactant self-assembly into vesicles

It is known that SDBS molecule can aggregate into global micelles in aqueous solution at the concentration above critical

micelle concentration (cmc). The cmc value of SDBS solution is about 2.0 mM as indicated from fluorescent probe technique in Fig. S1. With the addition of benzylamine hydrochloride (BzCl), the freshly prepared solution turns into bluish as shown in turbidity curve (Fig. S2). The SDBS/BzCl solution is investigated by combined techniques of cryo-TEM, confocal laser scanning microscopy (CLSM), fluorescence, and ζ-potential. Cryo-TEM evidences the existence of unilamellar vesicles with 100–200 nm diameters in the SDBS/BzCl (10 mM/2 mM) system (Fig. 1a). The thickness of vesicle bilayer is about 4–6 nm. Confocal laser scanning microscopy (CLSM) results with Nile Red as a fluorescent dye indicate the formation of unilamellar vesicles as large as ~1000 nm in diameters (Fig. 1b). Since the desirable thickness of a cryo-TEM specimen is less than 300 nm [38,39], objects quite large in all three dimensions (such as giant liposomes) cannot be imaged by cryo-TEM. In contrast, CLSM images only "see" the large objects. Therefore, cryo-TEM detects small vesicles (100–200 nm) while CLSM detects larger vesicles ranging from several hundred nanometers to micrometers. It is worthwhile that SDBS/BzCl vesicles are formed in the presence of low concentration of hydrotropic salt (2 mM BzCl for 10 mM SDBS). In literatures, however, surfactant vesicles are usually observed only when hydrotropic salt concentration is relatively high [27,40]. When the BzCl concentration increases further, unilamellar vesicles transform into multilamellar vesicles in SDBS/BzCl system (10 mM/10 mM). Fig. 2a gives the images of multilamellar vesicles with 200 nm diameters, in which the inter-bilayer distance is about 28 nm and the thickness of each surfactant bilayer is 4–6 nm. From the calculation of 50 vesicles in cryo-TEM, the vesicular inter-bilayer distance ranges from 20 nm to 40 nm with the average of 31 nm. In CLSM, multilamellar vesicles as large as several micrometers are clearly observed in fluorescence mode (Fig. 2b).

It is obvious that hydrotropic salt BzCl plays an essential role in the self-assembly process of surfactant solution, which can be explained by the theory of critical packing parameter. As raised Israelachvili, the molecular packing parameter is defined as $p = v_0/al_0$, where v_0 and l_0 are the volume and length of surfactant hydrophobic tail and a is the area of surfactant headgroup at the interface of hydrophobic core-hydrophilic media [41]. According to previous studies, hydrotropic salts can penetrate into surfactant aggregate with the ionic groups strongly binding to surfactant headgroups and the aromatic rings oriented between hydrocarbon tails [6,10,42,23,43,22]. In this work, the penetration of BzCl into surfactant aggregates can be reflected from the variation of chemical shift of $-CH_2-$ on BzCl in ^1H NMR spectra (Fig. 3). The chemical shift of $-CH_2-$ proton of BzCl is 4.05 ppm in BzCl solution (Fig. 3b) which changes to 3.70 ppm in SDBS/BzCl (10 mM/10 mM) solution (Fig. 3c). This indicates $-CH_2-$ proton undergoes from a polar environment to a relatively apolar environment. This can be rationalized that $-CH_2-$ proton is exposed to the bulk water

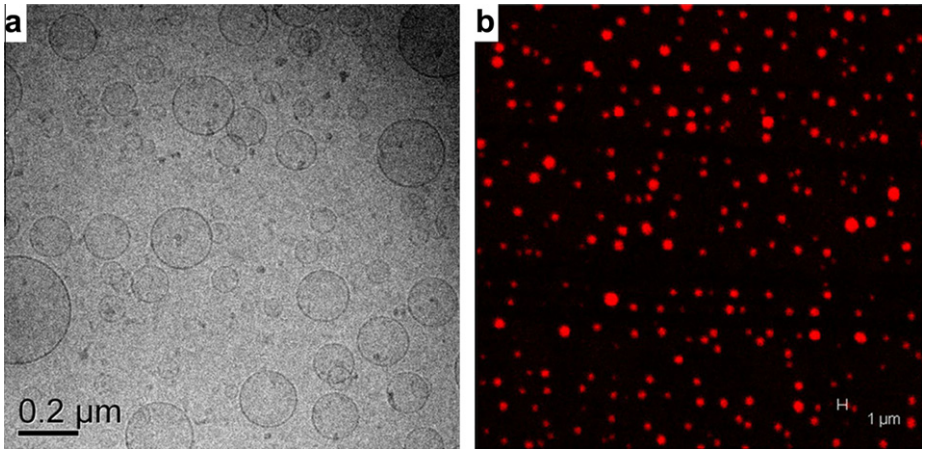

Fig. 1. Unilamellar vesicles formed in the system of SDBS/BzCl solution (10 mM/2 mM): (a) cryo-TEM image. (b) CLSM image stained with Nile Red in fluorescence mode. The images were taken 24 h after surfactant solutions were prepared.

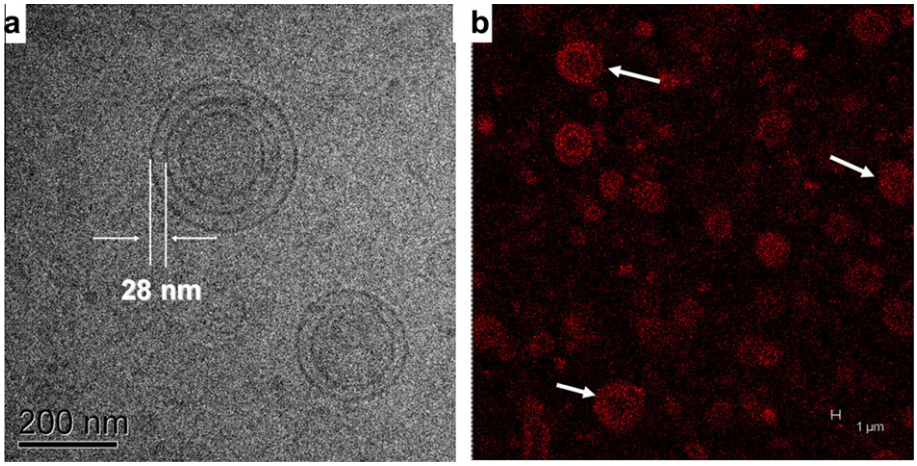

Fig. 2. Multilamellar vesicles formed in the system of SDBS/BzCl solution (10 mM/10 mM): (a) Cryo-TEM image; (b) CLSM image stained with Nile Red in fluorescence mode. The images were taken 24 h after surfactant solutions were prepared.

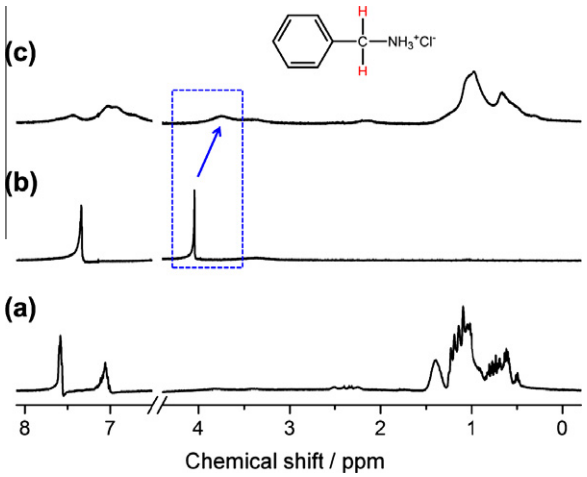

Fig. 3. ^{1}H NMR spectra of (a) 10 mM SDBS; (b) 10 mM BzCl; (c) SDBS/BzCl (10 mM/10 mM) solution in D_2O.

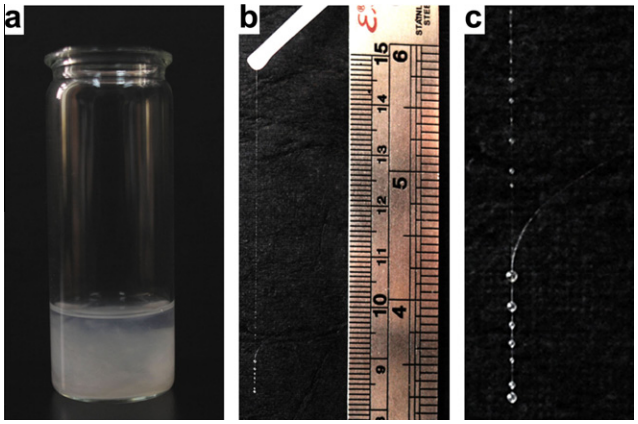

Fig. 5. (a) Macroscopic appearance of SDBS/BzCl solution that is kept for 6 months; (b) ultralong fibers lifted up from the SDBS/BzCl solution (a ruler is also placed on the right to indicate the length of surfactant fiber); (c) water droplets spreading on ultralong fibers. The fibers were prepared in SDBS/BzCl solution of 10 mM/10 mM.

in BzCl solution and experienced a polar environment; in the presence of SDBS, BzCl strongly binds to SDBS headgroup with the aromatic ring penetrating into SDBS hydrocarbon chains layer. In other words, $-CH_2-$ proton undergoes from a polar environment to an apolar environment and consequently the NMR signal shifted to upfield [6,44]. On the other hand, the signals are broaden and unresolved in the NMR spectra of SDBS/BzCl solution because the molecular motion of hydrotropic salt is restricted [6,45]. This further confirms the penetration of BzCl into SDBS aggregates.

Benefitting from the penetration of BzCl into surfactant aggregates, the electrostatic repulsion between surfactant headgroups can be greatly screened, and the close packing of surfactant molecules is expected. Besides, the incorporation of aromatic groups can contribute to the enhancement of hydrophobicity. As a consequence, the addition of BzCl greatly reduces the mean area of surfactant headgroups at the interface of the hydrophobic core-hydrophilic media, which ultimately increases the molecular packing parameter and induce the transformation from micelles to vesicles at low BzCl concentration. The molecular packing inside surfactant aggregates accompanied by micelle–vesicle transition is reflected by Nile Red fluorescence. In hydrophobic environments, Nile Red fluorescence intensity is much stronger, and its emission peak shifts to a shorter wavelength [46,47]. As shown in Fig. 4a, the addition of BzCl into 10 mM SDBS solution results into significant change in fluorescence emission. There is an abrupt decrease in λ_{em} and an increase in fluorescence intensity in SDBS solution with the addition of 2 mM BzCl (Fig. 4b), which is corresponding to unilamellar vesicles formation. This strongly suggests that the surfactant packing in the aggregates becomes more close when hydrotropic salt (BzCl) is added. As the concentration of BzCl is further increased, multilamellar vesicles are observed (Fig. 2). This is because when the BzCl concentration is close to or higher than that of SDBS, vesicular inter-bilayered repulsive forces are effectively reduced and multilamellar vesicles are facilitated.

3.2. Multilamellar vesicles transform into ultralong fibers

When the SDBS/BzCl solution (10 mM/10 mM) is kept at 23 °C for more than 6 months, a large amount of silky fibers precipitate from the aqueous solution as shown in Fig. 5a. It is amazing that the fibers are several centimeters in length which can be seen by naked eyes. However, it should be aware that the fibers in Fig. 5b may be a bundle of fibers but not an individual fiber. The surface of the organic fibers is hydrophilic as indicated by the spreading of many water droplets (Fig. 5c). Optical microscopic picture indicates the self-assembled fibers are highly flexible in solution and can be easily bent without obvious structural damage (Fig 6a). However, dry fibers are extremely fragile and hydration of the dry fibers can restore their flexibility (Fig. S3). The fibers under optical microscopy can extent to at least tens of micrometers. Transmission electronic microscopy (TEM) and scanning electronic microscopy (SEM) image shows the self-assembled 1D structures are not hollow tubes but solid fibers with the diameters ranging from 100 nm to 300 nm (Figs. 6b and S4). Further experiment

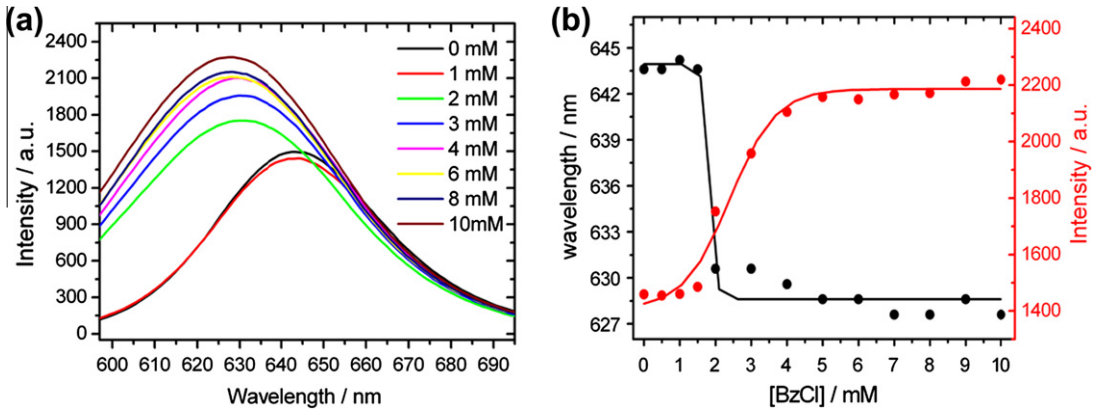

Fig. 4. (a) Fluorescence emission curve; (b) maximum emission wavelength and fluorescence intensity of Nile Red in the SDBS/BzCl solution. The concentration of Nile Red is 2.5 μM. The SDBS concentration is fixed at 10 mM and the BzCl concentration is varied from 0 to 10 mM.

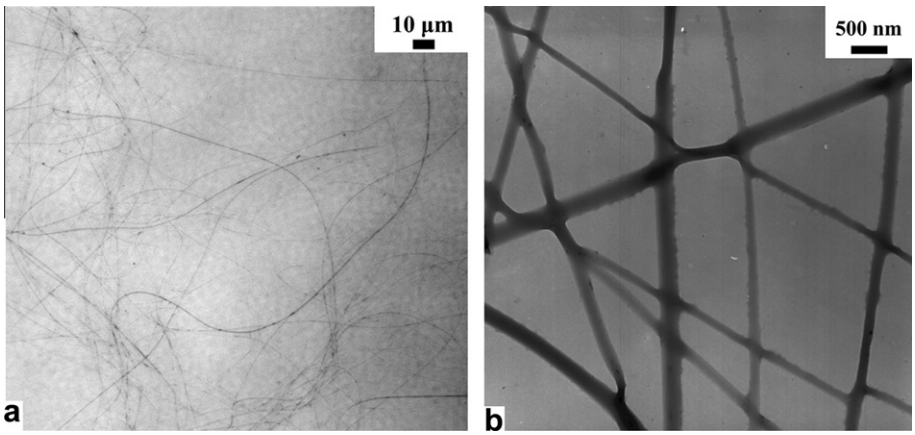

Fig. 6. (a) Optical and (b) TEM image of ultralong fibers in SDBS/BzCl solution (10 mM/10 mM).

reveals that self-assembled ultralong fibers can be formed in a series of SDBS/BzCl solution, in which the BzCl concentration is larger than SDBS concentration (Fig. 7).

To the best of our knowledge, most of the reported self-assembled 1D structure is formed in supramolecular solution or gel network, which cannot be isolated from aqueous or organic surroundings. The ultralong fibers in SDBS/BzCl system are found to be of high robustness that they can be conveniently collected by filtration or centrifugation, then washed by water and dried in the air. As shown in Fig. 5, the fibers can be lifted up from surfactant solution. This property allows us to obtain separated and purified fibers from solution, which is of significant importance for further applications in related fields. Besides, these self-assembled organic fibers are rather stable against dilution. When the isolated fibers are diluted by a large amount of water or re-dispersed in pure water, they are stable for more than 2 years without dissociation. This indicates the intermolecular interactions between SDBS and BzCl are strong enough to prevent fiber dissociation in aqueous surroundings.

Small- and wide-angle X-ray diffraction is performed to give molecular packing information inside the fibers at molecular scale (Fig. 8a). A strong diffraction peak ($2\theta = 3.78^\circ$) along with higher-order reflection peaks ($2\theta = 7.48^\circ$ and 11.18°) could be observed, which demonstrates the existence of well-ordered lamellar structures. According to the Bragg equation, the layer spacing corresponding to the first peak at the lowest 2θ value is calculated to be 23.4 Å. Wide-angle XRD shows sharp reflection peak at $2\theta = 22.48^\circ$ corresponding to the *d*-space of 3.95 Å, which is

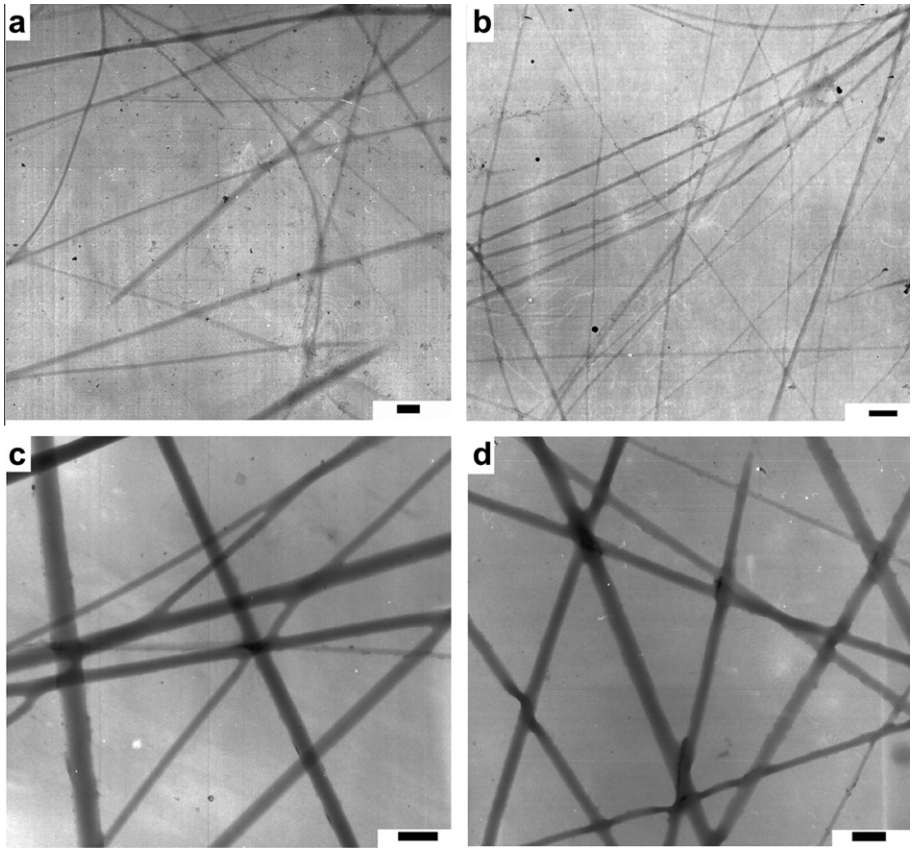

Fig. 7. Unstained TEM images of self-assembled fibers in SDBS/BzCl mixtures at the concentration of: (a) 5 mM/5 mM; (b) 5 mM/10 mM; (c) 10 mM/15 mM; (d) 10 mM/20 mM. The scale bars in the TEM images are 500 nm.

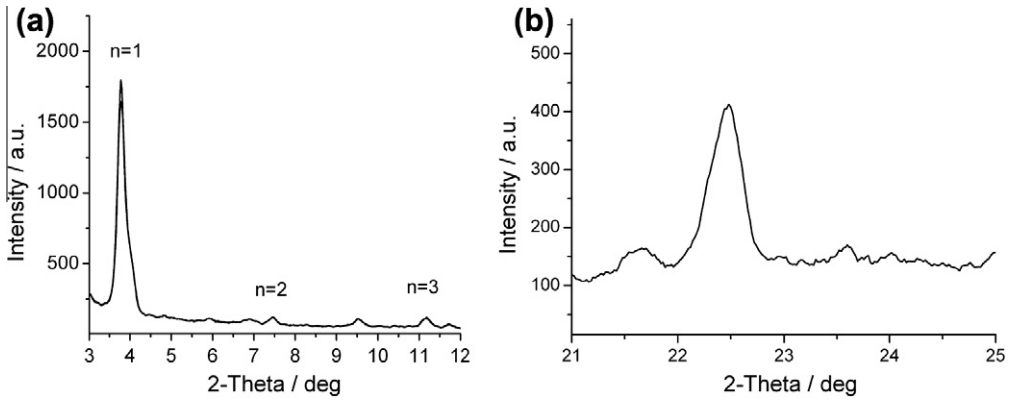

Fig. 8. (a) Small-angle and (b) wide-angle X-ray diffraction of fibers isolated from SDBS/BzCl (10 mM/10 mM) solution after centrifuging and washing three times with water.

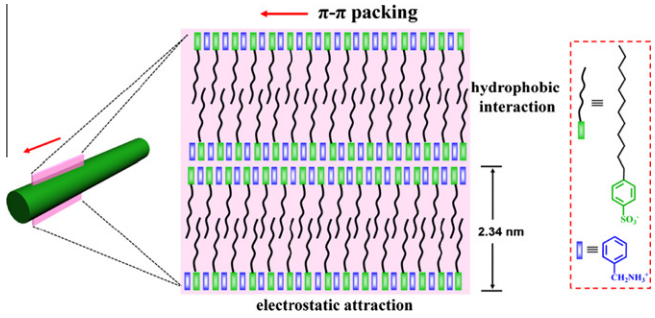

Fig. 9. Possible molecular packing model of lamellar structures in SDBS/BzCl fibers. The red arrows indicate the direction of π–π stacking. (For interpretation of the references to color in this figure legend, the reader is referred to the web version of this article.)

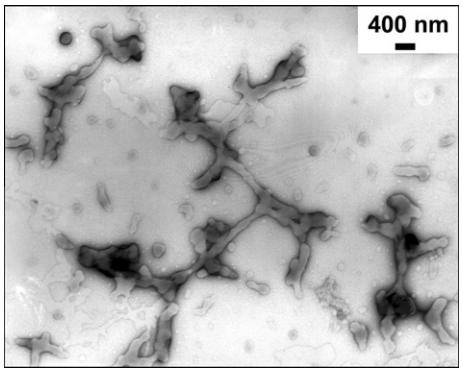

Fig. 10. TEM images of SDBS/BzCl (10 mM/10 mM) solution after sample preparation for 1 month. The picture clearly shows the vesicle aggregation and vesicle fusion.

comparable with the distance of π–π interactions (Fig. 8b) [48–51]. It is suggested this reflection peak may be ascribed to the well-ordered aromatic stacking between phenyl rings of SDBS and BzCl. Besides, elemental analysis discloses that the fibers are composed of dodecylbenzene sulfonate and benzylamine with 1:1 molar ratio. Based on these results and discussions, a possible molecular packing model of SDBS/BzCl nanofibers is proposed (Fig. 9). First, π–π stacking between SDBS and BzCl along the fiber axial direction (indicated by the arrow) provides the directional driving force for one-dimensional fiber growth. Second, surfactants adapt lamellar arrangement with the inter-layered space of 2.34 nm (calculated from small-angle XRD) inside the cross-section as indicated by pink rectangle in Fig. 9. Since the inter-layered distance is obviously less than twice the extended molecular length of SDBS (the molecular length of SDBS is approximately 2.0 nm), it can be imagined that SDBS may maintain an interdigitated or tilted bilayered structure (Fig. 9). Meanwhile, SDBS and BzCl interact strongly with each other and form 1:1 molecular pair, which are driven by electrostatic attractions between oppositely charged ionic groups, hydrophobic effect of surfactant hydrocarbon chains, and π–π interactions between phenyl groups of SDBS and BzCl. These non-covalent interactions are also believed to be responsible for the high robustness of ultralong fibers.

The transformation from vesicles to fibers is only observed in the SDBS/BzCl system where BzCl concentration is larger than that of SDBS and vesicle surface charge density is relatively low (Fig. S5). The macroscale fibers in SDBS/BzCl mixtures at the concentration of 5 mM/5 mM, 5 mM/10 mM, 10 mM/15 mM, and 10 mM/20 mM are shown in Fig. 7. It is therefore suggested that the generation of self-assembled ultralong fibers may be a consequence of vesicles aggregation. The speculation can be supported by TEM image in SDBS/BzCl (10 mM/10 mM) solution taken 1 month after sample preparation, in which vesicle aggregation and vesicle fusion can be noticed (Fig. 10). Additional molecular rearrangement may occur to repel the water out of vesicular core, and finally give birth to solid fibers rather than hollow structures. According to the above suggestions, the reduction of vesicle surface charge density is indispensable at the initial stage of vesicle aggregation. This can explain why ultralong fibers are only obtained in SDBS/BzCl system where BzCl concentration is larger than that of SDBS.

4. Conclusions

In conclusion, a hydrotropic salt (BzCl) is proven to facilitate molecular self-assembly of surfactant SDBS into unilamellar and multilamellar vesicles. Particularly, multilamellar vesicles are found to transform into ultralong fibers. These macroscopic fibers can be isolated from surfactant solutions and purified by washing. It is proposed that the formation of self-assembled ultralong fibers is owing to the aggregation of multilamellar vesicles and subsequent molecular rearrangement. The strong intermolecular interactions (i.e., hydrophobic effect, electrostatic attractions, and π–π interactions) are accounted for the self-organized aggregates, in which π–π interactions provide the directional forces for 1D fiber growth.

Although the concept of surfactant/hydrotropic salt self-assembly is not new [8,11,14], the results in this work are interesting and instructive. In literatures, surfactant/hydrotropic salt mixtures have the tendency to aggregate into rodlike or wormlike micelles

[5,10,25,22,52]; in some cases that vesicles or lamellar structures are formed, relatively high concentration of hydrotropic salt is required [27,40,53]. In SDBS/BzCl system, however, vesicles are observed at very low hydrotropic salt concentration (e.g., 2 mM BzCl for 10 mM SDBS). On the other hand, previously reported surfactant/hydrotropic salt systems tend to form nanoscale micelles or vesicles. However, SDBS/BzCl self-organizes into macroscale ultralong fibers. These two results show that BzCl can efficiently promote SDBS self-assemble into higher-ordered structures (i.e., vesicles and fibers). The extraordinary phenomena are ascribed to the enhanced intermolecular interactions between SDBS and BzCl, especially the additional π–π interactions. This work suggests that ordered aggregates or even macroscale structures can be fabricated in surfactant/hydrotropic salt systems by enhancing intermolecular interactions. It is also realized that the roles of versatile hydrotropic salts in surfactant solutions still need to be explored [11–13].

Acknowledgments

This work is supported by National Natural Science Foundation of China (20873001, 50821061, and 21073006) and National Basic Research Program of China (Grant No. 2007CB936201).

Appendix A. Supplementary material

Turbidity data, TEM image, SEM image, ζ potentials, and conductivity curve of SDBS/BzCl solution. Supplementary data associated with this article can be found, in the online version, at doi:10.1016/j.jcis.2011.11.067.

References

[1] S. Svenson, Curr. Opin. Colloid Interface Sci. 9 (2004) 201.
[2] J.C. Hao, H. Hoffmann, Curr. Opin. Colloid Interface Sci. 9 (2004) 279.
[3] H. Hoffmann, K. Horbaschek, F. Witte, J. Colloid Interface Sci. 235 (2001) 33.
[4] E.W. Kaler, A.K. Murthy, B.E. Rodriguez, J.A.N. Zasadzinski, Science 245 (1989) 1371.
[5] T. Shikata, H. Hirata, T. Kotaka, Langmuir 3 (1987) 1081.
[6] T. Shikata, H. Hirata, T. Kotaka, Langmuir 4 (1988) 354.
[7] R. Zana, Adv. Colloid Interface Sci. 57 (1995) 1.
[8] K. Trickett, J. Eastoe, Adv. Colloid Interface Sci. 144 (2008) 66.
[9] S.J. Candau, E. Hirsch, R. Zana, J. Colloid Interface Sci. 105 (1985) 521.
[10] P.A. Hassan, S.R. Raghavan, E.W. Kaler, Langmuir 18 (2002) 2543.
[11] T.K. Hodgdon, E.W. Kaler, Curr. Opin. Colloid Interface Sci. 12 (2007) 121.
[12] J. Eastoe, M.H. Hatzopoulos, P.J. Dowding, Soft Matter 7 (2011) 5917.
[13] M.H. Hatzopoulos, J. Eastoe, P.J. Dowding, S.E. Rogers, R. Heenan, R. Dyer, Langmuir 27 (2011) 12346.
[14] R. Abdel-Rahem, Adv. Colloid Interface Sci. 141 (2008) 24.
[15] T.M. Clausen, P.K. Vinson, J.R. Minter, H.T. Davis, Y. Talmon, W.G. Miller, J. Phys. Chem. 96 (1992) 474.
[16] Y.Y. Lin, Y. Qiao, Y. Yan, J.B. Huang, Soft Matter 5 (2009) 3047.
[17] B.D. Frounfelker, G.C. Kalur, B.H. Cipriano, D. Danino, S.R. Raghavan, Langmuir 25 (2009) 167.
[18] J.F. Berret, S. Lerouge, J.P. Decruppe, Langmuir 18 (2002) 7279.
[19] L.J. Magid, J.C. Gee, Y. Talmon, Langmuir 6 (1990) 1609.
[20] E. Mendes, J. Narayanan, R. Oda, F. Kern, S.J. Candau, C. Manohar, J. Phys. Chem. B 101 (1997) 2256.
[21] V.K. Aswal, J. Phys. Chem. B 107 (2003) 13323.
[22] D. Yu, X. Huang, M. Deng, Y. Lin, L. Jiang, J. Huang, Y. Wang, J. Phys. Chem. B 114 (2010) 14955.
[23] D. Kabir ud, W. Fatma, Z.A. Khan, A.A. Dar, J. Phys. Chem. B 111 (2007) 8860.
[24] W. Brown, K. Johansson, M. Almgren, J. Phys. Chem. 93 (1989) 5888.
[25] Y.Y. Lin, X. Han, J.B. Huang, H.L. Fu, C.L. Yu, J. Colloid Interface Sci. 330 (2009) 449.
[26] L. Zhai, B. Herzog, M. Drechsler, H. Hoffmann, J. Phys. Chem. B 110 (2006) 17697.
[27] M. Singh, C. Ford, V. Agarwal, G. Fritz, A. Bose, V.T. John, G.L. McPherson, Langmuir 20 (2004) 9931.
[28] B. Jing, X. Chen, Y. Zhao, X. Wang, F. Ma, X. Yue, J. Mater. Chem. 19 (2009) 2037.
[29] J.H. Fuhrhop, W. Helfrich, Chem. Rev. 93 (1993) 1565.
[30] R. Oda, I. Huc, M. Schmutz, S.J. Candau, F.C. MacKintosh, Nature 399 (1999) 566.
[31] Y. Qiao, Y.Y. Lin, Y.J. Wang, Z.Y. Yang, J. Liu, J. Zhou, Y. Yan, J.B. Huang, Nano Lett. 9 (2009) 4500.
[32] Y.Y. Lin, A.D. Wang, Y. Qiao, C. Gao, M. Drechsler, J.P. Ye, Y. Yan, J.B. Huang, Soft Matter 6 (2010) 2031.
[33] T. Shimizu, M. Masuda, H. Minamikawa, Chem. Rev. 105 (2005) 1401.
[34] Y.N. Xia, P.D. Yang, Y.G. Sun, Y.Y. Wu, B. Mayers, B. Gates, Y.D. Yin, F. Kim, Y.Q. Yan, Adv. Mater. 15 (2003) 353.
[35] T. Scheibel, Curr. Opin. Biotechnol. 16 (2005) 427.
[36] F.M. Menger, S.J. Lee, J. Am. Chem. Soc. 116 (1994) 5987.
[37] D.Y. Yan, Y.F. Zhou, J. Hou, Science 303 (2004) 65.
[38] J.R. Bellare, H.T. Davis, L.E. Scriven, Y. Talmon, J. Electron Microsc. Tech. 10 (1988) 87.
[39] Y.I. Gonzalez, E.W. Kaler, Curr. Opin. Colloid Interface Sci. 10 (2005) 256.
[40] R. Abdel-Rahem, H. Hoffmann, J. Colloid Interface Sci. 312 (2007) 146.
[41] J.N.M. Israelachvili, D.J. Ninhem, B.W., J. Chem. Soc., Faraday Trans. 2 72 (1976) 1525.
[42] R. Abdel-Rahem, M. Gradzielski, H. Hoffmann, J. Colloid Interface Sci. 288 (2005) 570.
[43] Y.Y. Lin, X.H. Cheng, Y. Qiao, C.L. Yu, Z.B. Li, Y. Yan, J.B. Huang, Soft Matter 6 (2010) 902.
[44] M. Vermathen, P. Stiles, S.J. Bachofer, U. Simonis, Langmuir 18 (2002) 1030.
[45] R.A. Salkar, D. Mukesh, S.D. Samant, C. Manohar, Langmuir 14 (1998) 3778.
[46] D.L. Sackett, J. Wolff, Anal. Biochem. 167 (1987) 228.
[47] M.C.A. Stuart, J.C. van de Pas, J. Engberts, J. Phys. Org. Chem. 18 (2005) 929.
[48] W. Pang, S. Zhu, C. Xing, N. Luo, H. Jiang, S. Zhu, J. Fluorine Chem. 129 (2008) 343.
[49] M.D. Curtis, J. Cao, J.W. Kampf, J. Am. Chem. Soc. 126 (2004) 4318.
[50] E.A. Meyer, R.K. Castellano, F. Diederich, Angew. Chem., Int. Ed. 42 (2003) 1210.
[51] M. Kimura, N. Miki, D. Suzuki, N. Adachi, Y. Tatewaki, H. Shirai, Langmuir 25 (2008) 776.
[52] H. Rehage, H. Hoffmann, Mol. Phys. 74 (1991) 933.
[53] B.K. Mishra, S.D. Samant, P. Pradhan, S.B. Mishra, C. Manohar, Langmuir 9 (1993) 894.